A "slingshot" laser-driven acceleration mechanism of plasma electrons

Gaetano Fiore[1,4], Sergio De Nicola[3,4], Renato Fedele[2,4]

[1] Dip. di Matematica e Applicazioni, Università di Napoli "Federico II",
Complesso Universitario Monte Sant'Angelo, Via Cintia, 80126 Napoli, Italy

[2] Dip. di Fisica, Università "Federico II", Complesso MSA, Via Cintia, 80126 Napoli, Italy

[3] SPIN-CNR, Complesso MSA, Via Cintia, 80126 Napoli, Italy

[4] INFN, Sez. di Napoli, Complesso MSA, Via Cintia, 80126 Napoli, Italy

We briefly report on the recently proposed [1, 2] electron acceleration mechanism named "slingshot effect": under suitable conditions the impact of an ultra-short and ultra-intense laser pulse against the surface of a low-density plasma is expected to cause the expulsion of a bunch of superficial electrons with high energy in the direction opposite to that of the pulse propagation; this is due to the interplay of the huge ponderomotive force, huge longitudinal field arising from charge separation, and the finite size of the laser spot.

Keywords: Laser-plasma interactions, electron acceleration, magnetohydrodynamics

I. INTRODUCTION

Today ultra-intense laser-plasma interactions allow extremely compact acceleration mechanisms of charged particles to relativistic regimes, with numerous and extremely important potential applications in nuclear medicine (cancer therapy, diagnostics), research (particle physics, inertial nuclear fusion, optycs, materials science, structural biology,...), food sterilization, transmutation of nuclear wastes, etc. A prominent mechanism for electrons is the *Wake-Field Acceleration* (WFA) [3]: electrons are accelerated "surfing" a plasma wake wave driven by a short laser or charged particle beam within a low-density plasma sample (or matter to be locally completely ionized into a plasma by the beam, more precisely a supersonic gas jet), and are expelled just after the exit of the beam out of the plasma, behind and *in the same direction as the beam* (forward expulsion). WFA has proved to be particularly effective since 2004 in the socalled *bubble* (or *blowout*) regime; it can produce electron bunches of very good collimation, small energy spread and energies of up to hundreds of MeVs [4–6] or more recently even GeVs [7, 8].

In Ref. [1, 2] it has been claimed that the impact of a very short and intense laser pulse in the form of a pancake normally onto the surface of a low-density plasma may induce also the acceleration and expulsion of electrons *backwards* (*slingshot effect*), see fig. 1. A bunch of plasma electrons (in a thin layer just beyond the vacuum-plasma interface) first are displaced forward with respect to the ions by the positive ponderomotive force $F_p \equiv \langle -e(\frac{\mathbf{v}}{c} \times \mathbf{B})^z \rangle$ generated by the pulse (here $\langle \rangle$ is the average over a period of the laser carrier wave, $\mathbf{E}, \mathbf{B}$ are the electric and magnetic fields, $\mathbf{v}$ is the electron velocity, and $\hat{\mathbf{z}}$ is the direction of propagation of the laser pulse; re-

call that F_p is positive, negative when the modulating amplitude ϵ_s of the pulse respectively increases, decreases), then are pulled back by the electric force $-eE^z$ due to this charge displacement. If the electron density $\widetilde{n_0}$ is carefully chosen in the range where the plasma oscillation period T_H is about twice the pulse duration τ, then these electrons invert their motion when they are reached by the maximum of ϵ_s, so that the negative part of F_p adds to $-eE^z$ in accelerating them backwards; equivalently, the total work $W \equiv \int_0^\tau dt \, F_p v^z$ done by the ponderomotive force is maximal. Also, the radius R of the laser spot should be "small", for the pulse intensity - as well as the final energy of the expelled electrons escaping to $z \to -\infty$ - to be "large", but not so small that lateral electrons obstruct them the way out backwards. If $\tau \gg T_H$, which was the standard situation in laboratories until a couple of decades ago, $F_p v^z$ oscillates many times about 0, $W \simeq 0$, and the effect is washed out.

The very short pulse duration τ and expulsion time t_e, as well as huge nonlinearities, make approximation schemes based on Fourier analysis and related methods unconvenient. But recourse to full kinetic theory is not necessary: we show [2, 9] that in the relevant space-time region a MagnetoHydroDynamic (MHD) description of the impact is self-consistent, simple and predictive. The set-up is as follows. We describe the plasma as consisting of a static background of ions and a fully relativistic, collisionless fluid of electrons, with the system "plasma + electromagnetic field" fulfilling the Lorentz-Maxwell and the continuity Partial Differential Equations (PDE). For brevity, below we refer to the electrons' fluid element initially located at $\mathbf{X} \equiv (X, Y, Z)$ as to the "$\mathbf{X}$ electrons", and to the fluid elements with arbitrary X, Y and specified Z as the "Z electrons". We denote: as $\mathbf{x}_e(t, \mathbf{X})$ the position at time t of the $\mathbf{X}$ electrons, and
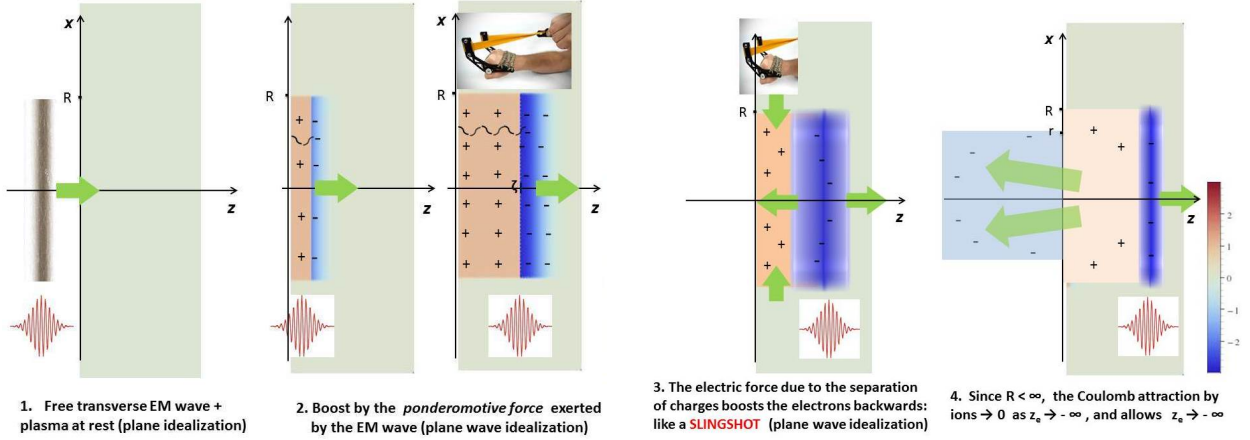
1. **Free transverse EM wave + plasma at rest (plane idealization)**

2. Boost by the *ponderomotive force* exerted by the EM wave (plane wave idealization)

3. The electric force due to the separation of charges boosts the electrons backwards: like a **SLINGSHOT** (plane wave idealization)

4. Since R < ∞, the Coulomb attraction by ions → 0 as z_e → - ∞ , and allows z_e → - ∞

FIG. 1. Schematic stages of the slingshot effect

for each fixed t as $\mathbf{X}_e(t,\mathbf{x})$ the inverse of $\mathbf{x}_e(t,\mathbf{X})$ [$\mathbf{x} \equiv (x,y,z)$]; as c the velocity of light; as m and as $n, \mathbf{v}, \mathbf{p}$ the electrons' mass and Eulerian density, velocity, momentum. $\boldsymbol{\beta} \equiv \mathbf{v}/c$, $\mathbf{u} \equiv \mathbf{p}/mc = \boldsymbol{\beta}/\sqrt{1-\boldsymbol{\beta}^2}$, $\gamma \equiv 1/\sqrt{1-\boldsymbol{\beta}^2} = \sqrt{1+\mathbf{u}^2}$ are dimensionless. We assume that the plasma is initially neutral, unmagnetized and at rest with electron (and proton) density $\widetilde{n_0}(z)$ depending only on z and equal to zero in the region $z < 0$. We schematize the laser pulse as a free transverse EM plane travelling-wave multiplied by a cylindrically symmetric "cutoff" function, e.g.

$$\mathbf{E}^\perp(t,\mathbf{x}) = \boldsymbol{\epsilon}^\perp(ct-z)\,\theta(R-\rho), \qquad \mathbf{B}^\perp = \hat{\mathbf{z}} \times \mathbf{E}^\perp \quad (1)$$

where $\rho \equiv \sqrt{x^2+y^2} \leq R$, θ is the Heaviside step function, and the 'pump' function $\boldsymbol{\epsilon}^\perp(\xi)$ vanishes outside some finite interval $0 < \xi < l$. Then, to simplify the problem,

1. The $R = \infty$ (i.e. *plane-symmetric*) version is studied first (section II.1), carefully choosing unknowns and independent variables. For sufficiently small densities and short times we can reduce the PDE's to a collection of decoupled *systems of two first order autonomous nonlinear ODE in Hamiltonian form*, which we solve numerically.

2. We determine (section II.2): $R < \infty$, $r > 0$ so that the plane version gives small errors for the surface electrons with $\rho \leq r \leq R$; the corresponding final energy, spectrum, etc. of the expelled electrons. For definiteness, we consider the $\widetilde{n_0}(z)$ of fig. 2.

We specialize our predictions to virtual experiments at the FLAME facility (LNF, Frascati). We invite for simulations (PIC, etc.) and experiments testing them.
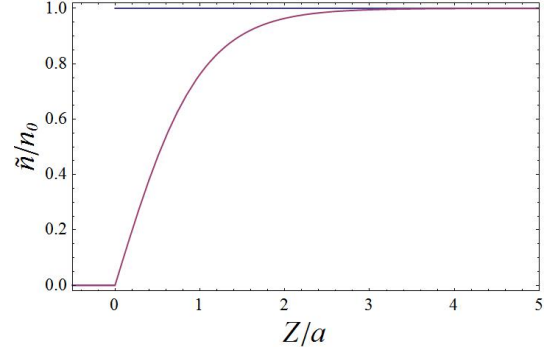

FIG. 2. The normalized $\widetilde{n_0}$ adopted here: step-shaped (blue) and continuous $\widetilde{n_0}(Z) = n_0\,\theta(Z)\tanh(Z/a)$, $a = 20\mu$m (purple); they respectively model the initial electron densities at the vacuum interfaces of an aerogel and of a gas jet (just outside the nozzle).

II.   THE MODEL

II.1.   Plane wave idealization

Our plane wave Ansatz reads: $A^\mu, \mathbf{u}, n-\widetilde{n_0}(z)$ depend only on z, t and vanish if $ct \leq z$; $\Delta\mathbf{x}_e \equiv \mathbf{x}_e - \mathbf{X}$ depends only on Z, t and vanishes if $ct \leq Z$. Then: $\mathbf{B} = \mathbf{B}^\perp = \hat{\mathbf{z}}\partial_z \wedge \mathbf{A}^\perp$, $c\mathbf{E}^\perp = -\partial_t\mathbf{A}^\perp$; the transverse component of the Lorentz equation implies $\mathbf{u}^\perp = e\mathbf{A}^\perp/mc^2$; by the Maxwell equations E^z is related to the longitudinal motion by

$$E^z(t,z) = 4\pi e\left\{ \widetilde{N}(z) - \widetilde{N}[Z_e(t,z)] \right\}, \widetilde{N}(Z) \equiv \int_0^Z d\eta\,\widetilde{n_0}(\eta), \tag{2}$$

what yields a conservative force on the electrons. For sufficiently small densities and short times the laser pulse is not significantly affected by the inter-

action with the plasma (the validity of this approximation is checked a posteriori [2]), and we can identify $\mathbf{A}^\perp(t,z) = \boldsymbol{\alpha}(\xi)$, $\xi \equiv ct-z$, where $\boldsymbol{\alpha}$ is the transverse vector potential of the "pump" free laser pulse. Hence also $\mathbf{u}^\perp(t,z) = e\boldsymbol{\alpha}(\xi)/mc^2$ is explicitly determined. For each fixed Z, the unknown $z_e(t,Z)$ appears in place of z in the equations of motion of the Z-electrons. But, as no particle can reach the speed of light, the map $t \mapsto \xi \equiv ct-z_e(t,Z)$ is strictly increasing, and we can use (ξ,Z) *instead of* (t,Z) as independent variables. It is also convenient to use the "electron s-factor" $s \equiv \gamma - u^z$ instead of u^z as an unknown, because it is *insensitive* to rapid oscillations of $\boldsymbol{\alpha}$, and $\gamma, \mathbf{u}, \boldsymbol{\beta}$ are *rational* functions of $\mathbf{u}^\perp, s$:

$$\gamma = \frac{1+\mathbf{u}^{\perp 2}+s^2}{2s}, \quad u^z = \frac{1+\mathbf{u}^{\perp 2}-s^2}{2s}, \quad \boldsymbol{\beta} = \frac{\mathbf{u}}{\gamma}. \quad (3)$$

Then the remaining PDE to be solved are reduced to the following collection of systems (parametrized by Z) of first order ODE's in the unknowns $\Delta(\xi,Z), s(\xi,Z)$:

$$\Delta' = \frac{1+v}{2s^2} - \frac{1}{2}, \quad s' = \frac{4\pi e^2}{mc^2}\left\{\widetilde{N}[\Delta+Z] - \widetilde{N}(Z)\right\} (4)$$

$$\Delta(0,Z) = 0, \qquad s(0,Z) = 1. \qquad (5)$$

Here $v(\xi) \equiv [e\boldsymbol{\alpha}(\xi)/mc^2]^2$, $\Delta \equiv z_e - Z$, $f' = \partial f/\partial \xi$. Eq.s (4) can be written also in the form [9] of *Hamilton equations* $q' = \partial H/\partial p$, $p' = -\partial H/\partial q$ in 1 degree of freedom: $\xi, -\Delta, s$ play the role of t, q, p. Solving (4-5) numerically all unknowns are determined. For $z>0$ $\mathbf{u}(t,z), n(t,z), ...$ evolve as forward travelling waves.

In particular, if $\widetilde{n_0}(Z) = n_0\theta(Z)$ then by (2) the longitudinal electric force acting on the Z-electrons is

$$\widetilde{F}_e^z(t,Z) = \begin{cases} -4\pi n_0 e^2 \Delta z_e = \text{elastic force} & \text{if } z_e > 0, \\ 4\pi n_0 e^2 Z = \text{constant force} & \text{if } z_e \leq 0; \end{cases}$$
$$(6)$$

hence as long as $z_e \geq 0$ each Z-layer of electrons is an independent copy of the *same* relativistic harmonic oscillator, (4-5) are Z-independent and reduce to a *single* system of two first order ODE's

$$\Delta' = \frac{1+v}{2s^2} - \frac{1}{2}, \qquad s' = M\Delta, \qquad (7)$$

$$\Delta(0) = 0, \qquad s(0) = 1, \qquad (8)$$

$(M \equiv 4\pi n_0 e^2/mc^2)$. $n_0 \to 0$ implies $s \equiv 1$, and the equations are solved in closed form [10, 11]. In fig. 3 we plot a typical pump and the corresponding solution of (7-8).
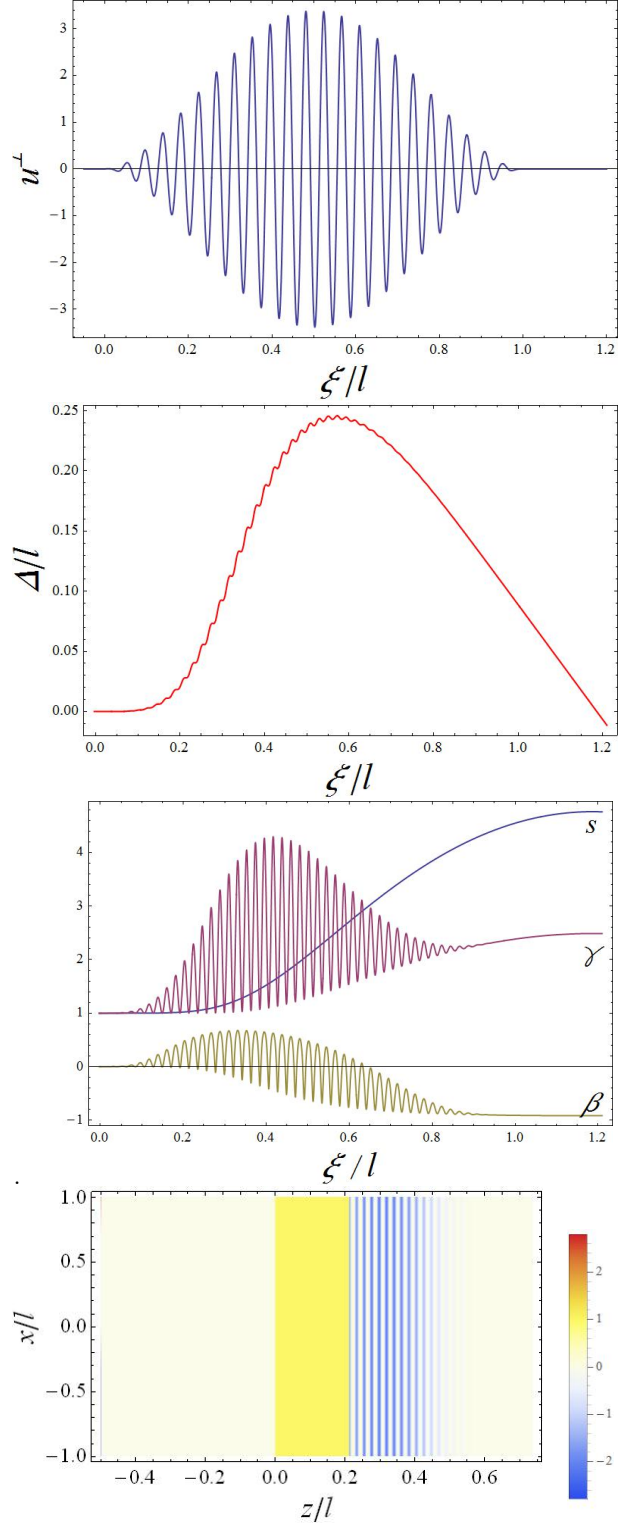

FIG. 3. Typical normalized pump amplitude $\mathbf{u}^\perp = e\boldsymbol{\alpha}/mc^2$ (vanishing outside $0 < \xi < l$), corresponding solution of (7-8) for $Ml^2 = 26$ and normalized charge density plot after 40 fs.
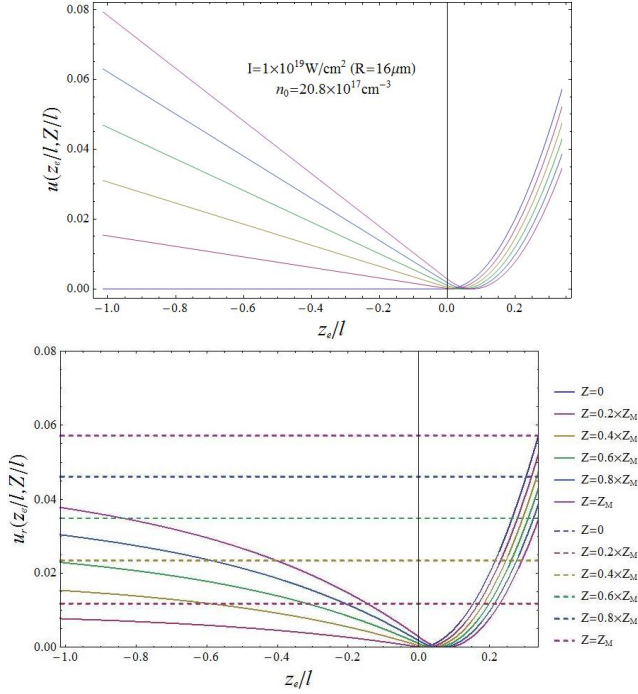
FIG. 4. Rescaled longitudinal electric potential energies in the idealized plane wave (up) and in the $r = 16\mu m$ (down) case, plotted as functions of z_e for $Z/Z_M = 0, .2, .4, .6, .8, 1$; the horizontal dashed lines are the left asymptotes of u_r for the same values of Z/Z_M.

II.2. Finite R corrections and experimental predictions

If $R < \infty$ the potential energies (parametrized by $Z > 0$) $U(z_e, Z)$ associated to (2) - due to charge separation - are inaccurate as $z_e \to -\infty$. We therefore replace $U \mapsto U_R$ in the equations of motion, where U_R is a suitable effective potential differing from U for $z_e < 0$; this allows $z_e(t, Z) \overset{t \to \infty}{\longrightarrow} -\infty$ (backward escape) for electrons in a suitable surface layer $0 \leq Z \leq Z_M$. If e.g. $\widetilde{n_0}(Z) = n_0 \theta(Z)$ then U, U_R (plot in fig. 4) are given by $U(z_e, Z) = 2\pi n_0 e^2 [\theta(z_e) z_e^2 - 2z_e Z + Z^2]$ and

$$U_R(z_e, Z) = \pi n_0 e^2 \Big[(z_e - 2Z)\sqrt{(z_e - 2Z)^2 + R^2} - 4Z z_e$$
$$+ R^2 \sinh^{-1}\frac{z_e - 2Z}{R} - z_e \sqrt{z_e^2 + R^2} - R^2 \sinh^{-1}\frac{z_e}{R}$$
$$+ 2Z^2 + 2Z\sqrt{4Z^2 + R^2} + R^2 \sinh^{-1}\frac{2Z}{R} \Big].$$

Solving the equations the map $\mathbf{X} \mapsto \mathbf{x}_e(t, \mathbf{X})$ turns out to be one-to-one for all t and for sufficiently small Z, showing the *self-consistency* of this MHD treatment. Some typical electron trajectories are shown in fig.'s 5, the animated versions are available at the hyperlink people.na.infn.it/~gfiore/slingshot-videos. The interplay of the ponderomotive, electric

forces yield the longitudinal forward and backward drifts at the basis of the slingshot effect. On the contrary, transverse oscillations due to $\mathbf{E}^\perp$ average to zero to yield vanishing final transverse drift and momentum, if - as usual - the pump (1) has a slow modulation ϵ_s in the support $0 < \xi < l$:

$$\boldsymbol{\epsilon}^\perp(\xi) = \hat{\mathbf{x}} \epsilon_s(\xi) \cos k\xi \qquad \text{with} \ \ |\epsilon_s'| \ll |k\epsilon_s| \quad (9)$$

(here the pump is polarized e.g. in the x-direction) implies $p^\perp(\xi) \simeq \epsilon_s(\xi) |\sin(k\xi) e/kc| = 0$ for $\xi \geq l$, and hence a good collimation of the expelled electrons. If the plasma is created by the impact on a supersonic gas jet (e.g. helium) of the pulse itself, then $l < \infty$ is the length of the interval where the intensity is sufficient to ionize the gas.

The EM energy $\mathcal{E}$ carried by a pulse (1), (9) is

$$\mathcal{E} \simeq \frac{R^2}{8} \int_0^l d\xi \, \epsilon_s^2(\xi). \qquad (10)$$

$\mathcal{E}$ is fixed and depends on the laser; reducing R (focalization) increases the intensity I, the electron penetration ζ and the slingshot force. But we need to tune R so that U_R be justified, i.e. the "information about the finite R" (contained in the retarded fields generated by charge separation) reach the $\vec{z}$-axis around expulsion time t_e (neither much earlier, nor much later). Moreover, R must be sufficiently large for the Forward Boosted Electrons (FBE) in an inner cylinder $\rho \leq r \leq R$ to be expelled before Lateral Electrons (LE), which are initially located outside the surface of the hole C_R created by the pulse and are attracted towards the $\vec{z}$-axis, obstruct their way out. These conditions amount to [1, 2]

$$\frac{[t_e - \bar{t}]c}{R} \sim 1, \quad r \equiv R - \frac{\zeta(t_e - l/c)}{2(t_e - \bar{t})} \, \theta(ct_e - l) > 0, \qquad (11)$$

which can be fulfilled also with a rather small R (here $\bar{t}$ is the time resp. of maximal penetration of the FBE).

We adopt a gaussian modulating amplitude

$$\epsilon_s^g(\xi) = b_g \exp\left[-\frac{(\xi - l/2)^2}{2\sigma} \right] \theta(\xi)\theta(l - \xi); \qquad (12)$$

the parameters $b_g, \sigma, l, \dots$ are determined by $\mathcal{E}, R$ and the full width at half maximum l' of the pulse. We report in table I and fig. 6 sample results of extensive numerical simulations performed using as inputs the parameters available [12] in virtual experiments at the FLAME facility of the Laboratori Nazionali di Frascati: $l' \simeq 7.5\mu m$ (corresponding to a time $\tau' = 25$fs), wavelength $\lambda \simeq 0.8\mu m$, $\mathcal{E} = 5$J, R tunable in the range $10^{-4} \div 1$cm; a supersonic helium jet or an aerogel (if $\widetilde{n_0}(Z) = n_0 \, \theta(Z)$ with
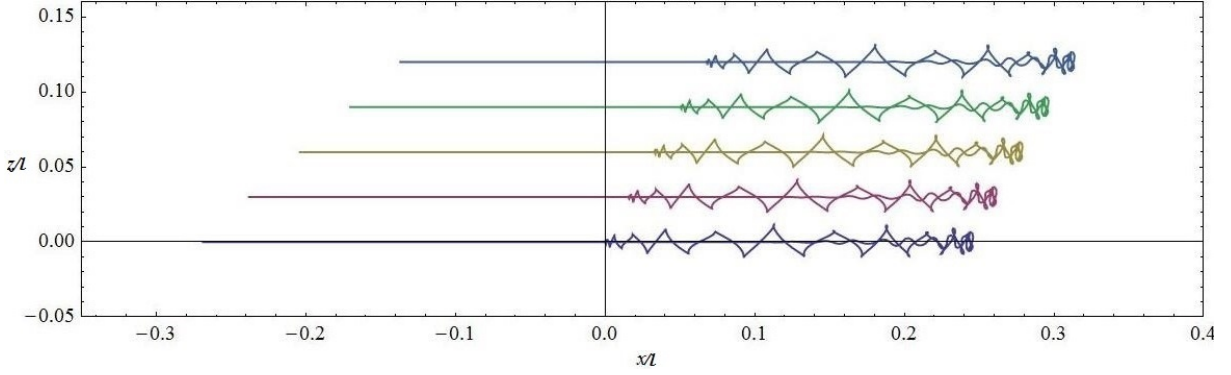
FIG. 5. Trajectories (after about 150 fs) of electrons initially located at $Z/Z_M = 0, 0.25, 0.5, 0.75, 1$ under the same conditions as in fig. 3.
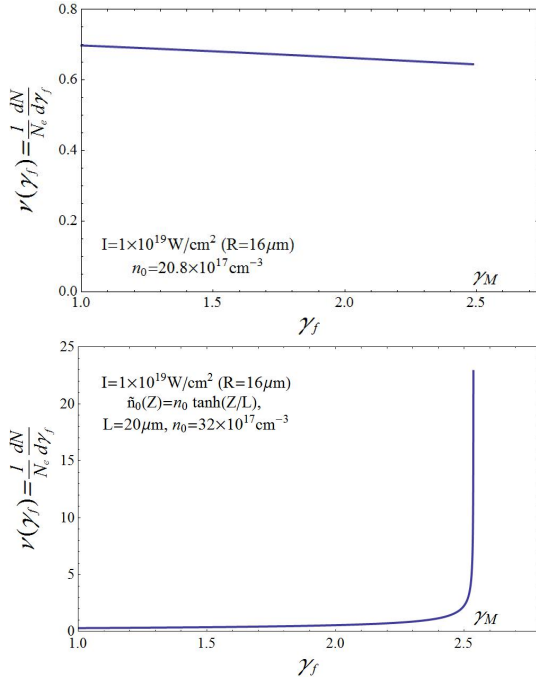

FIG. 6. Spectra of the expelled electrons for average pulse intensitiy $I = 10^{19}$ W/cm^2 and step-shaped (up) or continuous (down) $\widetilde{n_0}$.

most monochromatic) around γ_M, the maximal γ_f.

Summarizing, this new laser-induced "slingshot" acceleration mechanism should yield well-collimated bunches of electrons of energies up to few tens MeV. It is easily tunable and testable with present equipments.

pulse energy $\mathcal{E} \simeq 5$J, wavelength $\lambda \simeq .8\mu$m, duration $\tau' = 25$fs					
pulse spot radius $R\,(\mu$m$)$	16	8	4	2	2
average intensity $I\,(10^{19}$ W/cm$^2)$	1	4	16	64	64
asymptotic density $n_0(10^{19}$cm$^{-3})$	0.8	2	13	80	20
maximal relativistic factor γ_M	2.6	6	8.5	14	21
maximal expulsion energy(MeV)	1.3	3	4.4	7.2	11

pulse spot radius $R\,(\mu$m$)$	2	1
average intensity $I\,(10^{19}$ W/cm$^2)$	64	255
initial density $n_0(10^{19}$cm$^{-3})$	12	40
maximal relativistic factor γ_M	12.4	22.6
maximal expulsion energy(MeV)	6.4	11.5

TABLE I. Sample inputs and corresponding outputs if the target is: a supersonic helium jet (up) or an aerogel (down) with initial densities profiles as in fig. 2. The expelled charge is in all cases a few 10^{-10}C

$n_0 \gtrsim 48 \times 10^{18}$cm^{-3}) as targets. The energy spectrum, or equivalently the distribution $\nu(\gamma_f)$ of the expelled electrons as a function of their final relativistic factor, depends dramatically on $\widetilde{n_0}, R$; pleasantly, in the case $\widetilde{n_0}(Z) = n_0\, \theta(Z) \tanh(Z/a)$ it is peaked (al-

[1] G. Fiore, R. Fedele, U. de Angelis, Phys. Plasmas **21** (2014), 113105.
[2] G. Fiore, S. De Nicola, arXiv:1509.04656.
[3] T. Tajima, J.M. Dawson, *Phys. Rev. Lett.* **43** (1979), 267.
[4] S. P. D. Mangles, et al., *Lett. Nat.* **431** (2004), 535-

538.

[5] C. G. R. Geddes, et al., *Lett. Nat.* **431** (2004), 538-541.

[6] J. Faure, et al., Lett. Nat. **431** (2004), 541544.

[7] X. Wang, et al., *Nature Communications* **4**, Article nr: 1988.

[8] W. P. Leemans, et al., *Phys. Rev. Lett.* **113** (2014),

245002.

[9] G. Fiore, *A plane-wave model of the impact of short laser pulses on plasmas*, in preparation.

[10] G. Fiore, J. Phys. A: Math. Theor. **47** (2014), 225501.

[11] G. Fiore, Acta Appl. Math. **132** (2014), 261-271.

[12] L.A. Gizzi, *et al.*, *Appl. Sci.*, **3** (2013), 559-580.